# Unexpected collapses during isotropic consolidation of model granular materials

## Effondrements inattendus pendant la consolidation isotrope des milieux granulaires modèles

Thiep Doanh [a,*], Alain Le Bot [b], Nouha Abdelmoula [a], Lassad Gribaa [a], Stéphane Hans [a], Claude Boutin [a]

[a] École nationale des travaux publics de l'État, LGCB, LTDS (UMR 5513), Vaulx-en-Velin, France
[b] École centrale de Lyon, LTDS (UMR 5513), Écully cedex, France

## ARTICLE INFO

## ABSTRACT

This paper reports the unexpected instantaneous instabilities of idealized granular materials under simple isotropic drained compression. Specimens of monosized glass beads submitted to isotropic compression exhibit a series of local collapses under undetermined external stress with partial liquefaction, experience sudden volumetric compaction and axial contraction of various amplitude. Short-lived excess pore water pressure vibrates like an oscillating underdamped system in the first dynamic transient phase and rapidly disperses in the subsequent longer dissipation phase. However, very dense samples maintain a collapse-free behaviour below a threshold void ratio $e_{30}^{col}$ at 30 kPa of stress. The potential mechanisms that could explain these spontaneous collapses are discussed.

## RÉSUMÉ

Cet article concerne les instabilités instantanées et inattendues des milieux granulaires modèles en simple consolidation isotrope. Les échantillons de billes de verre monodisperses soumis à une compression isotrope montrent une série d'effondrements locaux à des contraintes externes indéterminées, avec une liquéfaction partielle, une compaction volumétrique et une contraction axiale d'amplitude variable. Les très courts excès de pression interstitielle vibrent comme un système oscillant sous-amorti pendant une première phase dynamique transitoire, puis rapidement se dispersent pendant une phase de dissipation plus longue. Néanmoins, les échantillons très denses en dessous d'un seuil

d'indice des vides $e_{30}^{col}$ à 30 kPa de contrainte sont exempts d'instabilités. Les mécanismes potentiels pouvant expliquer ces effondrements spontanés sont discutés.

## Version française abrégée

Un nouveau mode de liquéfaction en compression isotrope drainée a été découvert dans le cadre de nos travaux précédents sur une assemblée de grains idéalisés très lâches. Cet article explore les instabilités de type effondrement sur une plus large gamme de densités. L'objectif est de comprendre les mécanismes déclenchant ces instabilités et de proposer quelques explications plausibles quant aux origines physiques de ces instabilités que sont les effondrements, la liquéfaction et les frottements saccadés.

En consolidation isotrope des deux milieux granulaires modèles de la Fig. 1, au lieu d'avoir une compressibilité décroissante continue en fonction de la densité, les expériences réalisées avec une cellule triaxiale (Fig. 2), révèlent des sauts soudains et simultanés de déformations volumiques et axiales (Fig. 3). Ces sauts sont dus à une augmentation instantanée de la surpression interstitielle, qui peuvent être décomposés en deux phases. La première phase transitoire dure 200 ms ; durant celle-ci, la surpression interstitielle vibre comme un système oscillant sous-amorti avec une fréquence dominante d'environ 100 Hz (Fig. 4) ; elle est suivie d'une plus longue phase de dissipation pour revenir àà l'équilibre initial de contre-pression constante. Le coefficient d'anisotropie incrémentale mesuré, largement anisotrope (Fig. 6), montre que l'anisotropie structurale pourrait être un ingrédient majeur responsable des effondrements observés. Ces instabilités sont apparues à des contraintes isotropes indéterminées (Fig. 7), dans la gamme de 20 à 500 kPa. L'ensemble des expériences permet de montrer qu'il existe un seuil d'indice des vides $e_{30}^{col}$ à 30 kPa de contrainte, en dessous duquel ces instabilités disparaissent totalement (Fig. 8).

Il est conjecturé que l'anisotropie structurale initiale est responsable de l'anisotropie induite des dé-formations en consolidation isotrope, malgré un comportement quasi élastique (Fig. 9). La rupture des chaînes de forces, facilitée par le roulement des grains parfaitement sphériques, peut induire des dé-formations locales de cisaillement et provoque une augmentation de la surpression interstitielle dans un milieu totalement saturé, due à l'incompressibilité de l'eau. La présence du fluide est seulement un facteur aggravant. Il est probable que ces instabilités en consolidation isotrope et les frottements saccadés en cisaillement partagent les mêmes origines physiques.

## 1. Introduction

Granular materials are one of the most studied objects in civil engineering. However, despite a large number of intensive theoretical and experimental studies, many important aspects such as anisotropy, principal stress rotation, cyclic loading and liquefaction are not yet fully understood [1,2]. A possible explanation is the difficulty to relate the macroscopic mechanical parameters to the properties of sand grains [3]. One option is to use monodispersed spherical glass beads as model granular materials, together with discrete element method (DEM [4,5]) pioneered by [6] and popularized by [7], as an alternative way to explore and understand the complexity hidden in real soils.

Unexpectedly, triaxial compression shear tests on these idealized materials reveal diffuse instabilities, termed stick-slip [8–11], and leave many questions unanswered. For example, what happens during the mandatory isotropic consolidation preceding the triaxial tests? Granular experimentalists often overlook this first consolidation step.

Spontaneous instabilities during isotropic compression of very loose bead assemblies have been discovered in our previous work [12]. In some rare cases, a sudden increase in the interstitial pore pressure can lead to a new mode of liquefaction in *isotropic* and *drained* compression. The rapid and spontaneous collapse are therefore responsible for liquefaction.

In this paper, instead of focusing on these spectacular events, we systematically explore these spontaneous instabilities over a *large range of sample densities*. The objective is to better understand the underlying mechanisms behind these unexpected isotropic instabilities, and to offer some plausible explanations about the physical origin of the collapse, liquefaction, and stick-slip phenomena.

## 2. Experimental setup

The granular sample consists of a cylinder of monodisperse glass beads confined by a latex membrane and fully saturated by water. The cylinder has height $H_0 = 70$ mm, diameter $D_0 = 70$ mm and volume $V_0$. The mean diameter of glass beads is $d = 0.723$ mm, giving a slenderness $D_0/d \approx 100$, which is large enough to avoid boundary effects. The sample was isotropically compressed inside a triaxial system (Fig. 2). Compressed air was increased at 0.3 kPa/s to impose the total stress $\sigma$. The real-time experimental recordings consist in measuring synchronously $\sigma$, the pore-water pressure $U$, the axial strain $\varepsilon_a$, and the volumetric strain $\varepsilon_v$. A strain-gauge pressure sensor measured $\sigma$ inside the cell. $U$ was measured outside the triaxial cell at a distance of about 60 cm using a very thick plastic tube connected to the top cap of the granular sample; it is therefore slightly under-estimated. The axial displacement $\Delta h$ was measured inside the triaxial cell using a
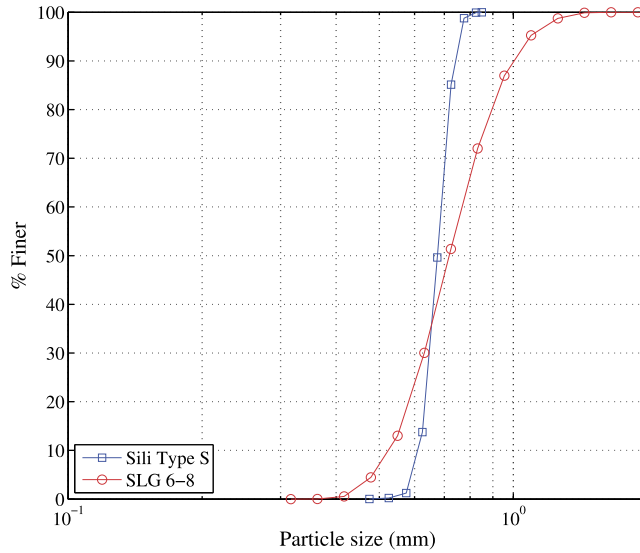
**Fig. 1.** Particle size distribution of SLG 6-8 and Sili Type S glass beads of 0.7 mm of mean diameter.
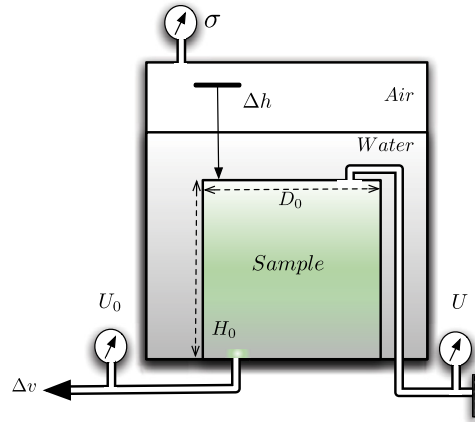


**Fig. 2.** Experimental setup for the isotropic compression of a short cylindrical granular sample inside a classical triaxial cell.

linear variable differential transformer sensor mounted directly on the top platen to estimate $\varepsilon_a = \Delta h/H_0$. The global water volume $\Delta v$ expelled from or moving into the sample was measured to determine $\varepsilon_v = \Delta v/V_0$.

The industrial soda lime spherical glass beads "Sil-glass SLG 6-8" used in this experimental study were commercialized by CVP, Linselles, France.[1] The grain size distribution in Fig. 1 using a particle size analyzer by laser diffraction indicates a clean and poorly graded fine-grained granular material with uniformity coefficient, $C_u = 1.463$, and curvature coefficient, $C_c = 0.989$. Only virgin glass was used to avoid potential wearing effects. Predetermined quantities of moist glass beads, mixed with 2% of distilled water in weight, were carefully placed and gently compacted in five layers of prescribed thickness inside a cylindrical and open-ended latex membrane of 0.3 mm to create very loose granular samples conforming to the modified moist tamping and under compaction technique. The $CO_2$ method together with deaerated distilled water and a constant back pressure $U_0$ of 200 kPa were used to obtain a quasi-saturated state, assessed by Skempton's coefficient $B$ higher than 0.95, before and after the test.

## 3. Results and analysis

A typical compressibility of very loose model granular materials is shown in Fig. 3a as variation of the void ratio $e = e_{30} - \varepsilon_v(1 + e_{30})$ versus $\sigma$, $e_{30}$ is $e$ at 30 kPa. Short black arrows indicate the time direction. Under imposed external stress, granular media such as sand exhibit normally a continuous increase in density [13,14]. However, instead of the expected
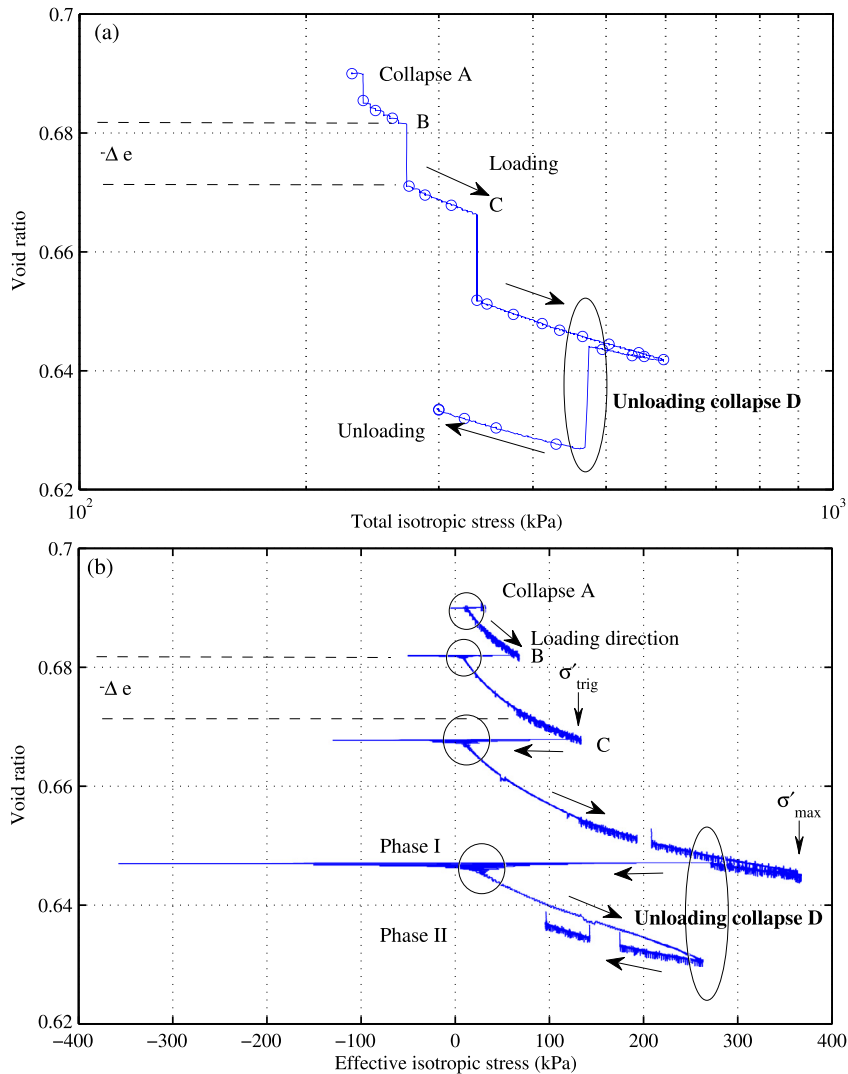
**Fig. 3.** (a) Void ratio vs. total isotropic stress. (b) Void ratio vs. effective isotropic stress. Spontaneous collapses and partial liquefaction under isotropic compression from 30 to 400 kPa, with $e_{30} = 0.690$.

smooth and continuous compaction, large unexpected drops $\Delta e$ in the void ratio can be seen. Between two events, the normal continuous decrease of $e$ is observed during the loading phase. Surprisingly, a drop in $e$ has also been noticed during the unloading process. The micro-structure presumably stable up to the maximum total stress reached during loading is actually unstable since additional collapses remain possible below this threshold. The rarity of unloading collapse suggests however a still metastable microstructure for an overconsolidated state.

The compressibility of the granular skeleton is revealed by introducing the effective stress $\sigma' = \sigma - U$ in Fig. 3b, with $U$ the actual pore pressure. The drops A to C in loading occur successively at $\sigma'_{\text{trig}} = 34$, 70 and 135 kPa, and the unloading drop D at 274 kPa. Each event consists of a sudden and simultaneous compressive volumetric strain (compaction), together with a reduction of $\sigma'$ due to a sudden surge $\Delta U = U - U_0$ of the pore water pressure, followed by a gradual recover of $\sigma'$. Note that at the beginning of each collapse, the effective stress takes negative values during a brief period of time of less than 100 ms. This means, following Terzaghi's effective stress principle, that a separation of beads occurs, but it is probably small and lasts during a too short period to lead to liquefaction.

The complete individual time evolution of various measurements can be seen in Fig. 4. The excess pore pressure $\Delta U$ was normalized by the brief stabilizing $\Delta U_{\text{stable}}$. The time origin is shifted to the beginning of the transient phase $\pm 0.5$ ms, which is the current time resolution.

The evolution of $\Delta U$ can be decomposed into two phases. First a fast transient phase $I$ (hollow circle in Fig. 3b) occurred within 200 ms at constant volume. $\Delta U$ vibrates like an oscillating underdamped system with a dominant frequency of about 100 Hz (Fig. 4). We have checked that this frequency is not a resonance of the pressure sensor (with a very stiff one). It also does not depend on the tube length by which the pressure sensor is connected to the sample (from 60 cm to 160 cm).
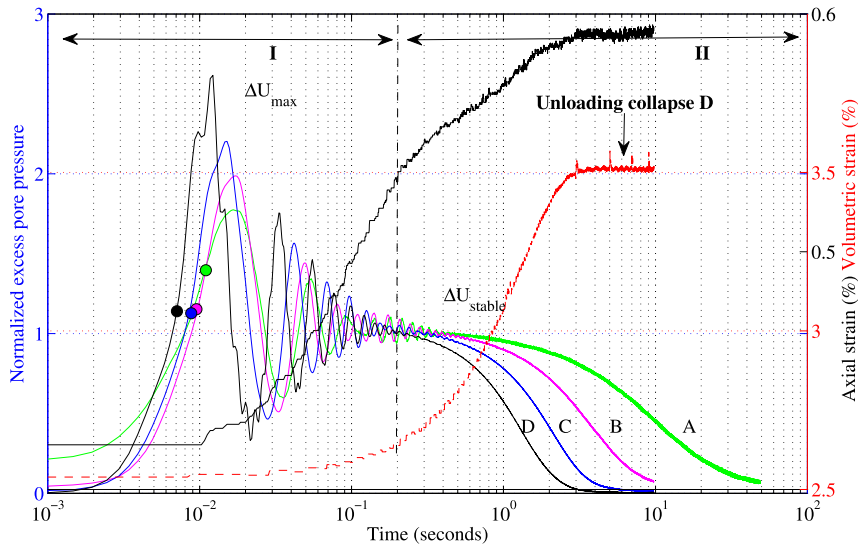
**Fig. 4.** Two phases of pore water pressure development of collapses at 33 (green), 70 (magenta), 135 (red), and 274 (black) kPa: I fast and transient development, II dissipation. The axial strain (black) and the volumetric strain (red) refer to the unloading event D. Referred liquefaction levels (solid circles) are indicated.

But it is not excluded that this frequency depends on the sample size, the mass of the top platen or even an artefact of the experimental setup by not yet identified components. The briefness of this phase should be compared with the slow loading rate; $\sigma$ is nearly constant during this phase and is not affected by the fluctuations of $U$. The solid circles indicate the level of null effective stress (liquefaction). The rising time to the first peak $\Delta U_{\max}$ is within 10 ms, followed by relatively fast decay to a stable value $\Delta U_{\text{stable}}$. Then it appears a long dissipation phase $II$ in which $\Delta U$ returns to the initial equilibrium $U = U_0$ at a nearly constant axial strain.

Fig. 4 also gives the time evolution of $\varepsilon_v$ and $\varepsilon_a$ only for the rare unloading collapse event D. It reveals a fast axial contraction up to 0.592% from 0.421% within only 2 s. It clearly indicates a dynamic regime of the collapse phenomenon. Similar observations apply for all collapses. Note a comparable dynamic regime in unloading for $\Delta U$ with surprising compressive axial and volumetric strains, however with the largest pore pressure generation and the smallest dissipation time.

The volumetric strain indicates an overall compaction of only 0.972% during collapse, with a larger initial time delay; its development is far behind that of the axial strain in terms of time evolution. Fig. 5 shows the complete evolution of $U$, $\sigma$, $\varepsilon_a$ and $\varepsilon_v$ for the total test duration. The narrow and surprisingly very sharp peaks of $U$ are clearly related to these events, despite the drainage system, and indicate a quite fast dissipation.

Since the internal pore pressure is not homogeneous, $\sigma'$ depends on the measurement position of $U$, but not the detection time of the collapse. So, only the magnitude of $\sigma'$ may be misestimated. However, if a partial liquefaction is detected by $U$, the event is stronger elsewhere.

### 3.1. Structural anisotropy

The static incremental anisotropy coefficient $i_{\text{sta}} = \Delta\varepsilon_v / \Delta\varepsilon_a$ is measured during the smooth phase between two collapses. It is found a more or less constant value of about 16, indicating a highly anisotropic structure, contrasting sharply the isotropic structure with $i \approx 3.0$ for loose laboratory sands (i.e. Hostun or Toyoura) created by the same moist-tamping procedure [15]. We may also introduce a dynamic anisotropy coefficient $i_{\text{dyn}} = \Delta\varepsilon_v / \Delta\varepsilon_a$, where $\Delta\varepsilon_v$ and $\Delta\varepsilon_a$ are estimated between the beginning and the very end of a collapse (after the pore pressure dissipation). It is found that both anisotropy coefficients are approximatively equal in Fig. 6, $i_{\text{dyn}} \approx i_{\text{sta}}$, showing their independence on the loading rate. This observation suggests that the anisotropic constitutive model may be independent of the time scale.

### 3.2. Macroscopic parameters

The occurring of isotropic triggering stress $\sigma'_{3\text{trig}}$ is randomly distributed in the studied range of 30 to 500 kPa; it can be as small as 33 kPa, without any preceding local collapses, or as large as 456 kPa, with numerous preceding local collapses or precursors.

Fig. 7 gives the relation between two characteristics of $\Delta U$ in the transient phase, $\Delta U_{\max}$ (hollow symbols) and $\Delta U_{\text{stable}}$ (solid symbols). While the short-lived $\Delta U_{\max}$ is often located above the diagonal red dash line representing the liquefaction state of null effective stress where $\Delta U$ equals the net total confining pressure $\sigma - U_0$, most of the stable value $\Delta U_{\text{stable}}$ remain below or near this line. One possible *speculated* explanation is that the brief duration of the transient phase *I*, below
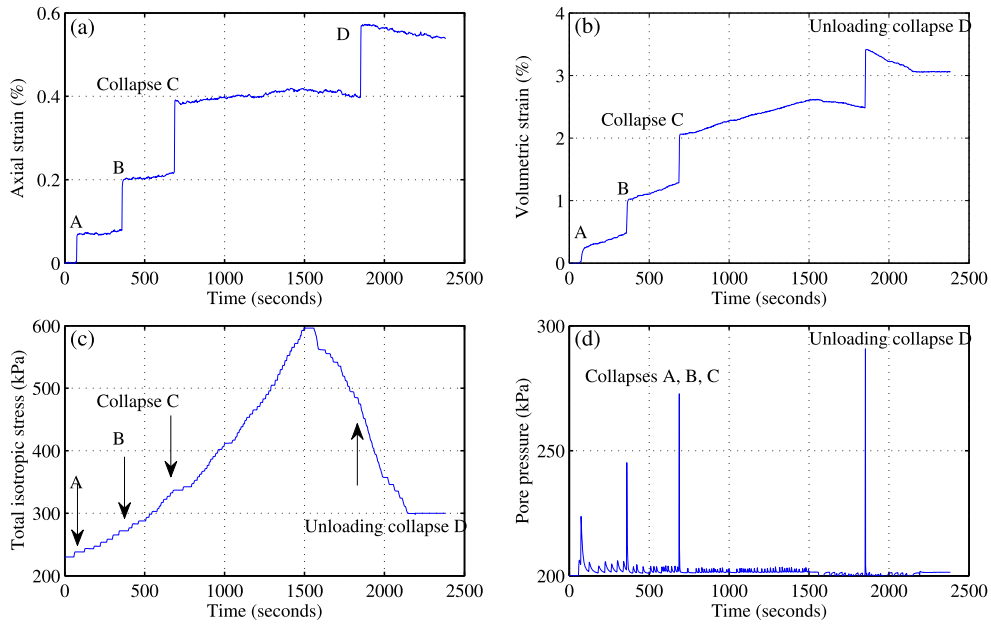
**Fig. 5.** Time evolution of axial strain $\varepsilon_a$ (a), volumetric strain $\varepsilon_v$ (b), total isotropic stress $\sigma$ (c), and pore pressure $U$ (d) versus time since the start of the isotropic compression. The vertical arrows in (c) indicate the onset of collapses on the evolution of the total isotropic stress.
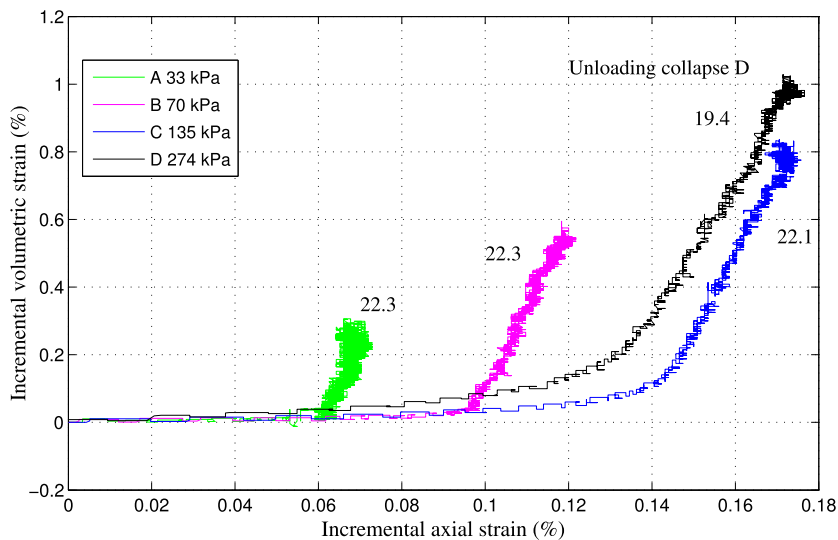


**Fig. 6.** Relationships between the incremental volumetric and axial strain developed during collapse events at 33 (green), 70 (magenta), 135 (red) and 274 (black) kPa. Superimposed black numbers indicate the measured dynamic incremental anisotropic coefficient $i_{\text{dyn}}$.

200 ms, is enough to generate locally the liquefaction, but not enough to sustain and spread out this liquefaction state to the whole sample. The stabilized value $\Delta U_{\text{stable}}$, located below the liquefaction line, gives a small but positive value of $\sigma'$, which is enough to prevent a global liquefaction.

By exploring various $e_{30}$, a threshold value $e_{30}^{\text{col}} = 0.590$ appears in Fig. 8. Samples with higher density (black circles) have no collapse (Fig. 9). It represents the transition from a discrete volumetric compaction created by local dynamic instability with partial liquefaction to a continuous one exempted from all changes in the pore pressure level. Logically, it is lower than the previously identified liquefaction-free threshold $e_{30}^{\text{liq}} = 0.690$ [12]. This threshold can be the physical attribute controlling the disappearance of collapses on dense samples during isotropic compression.

Isotropic collapse has been repeatedly and consistently observed in more than 85 experiments including other glass beads (green symbols in Figs. 7 and 8 for "Silibeads" with similar mean diameter, commercialized by Sigmund–Lindner,
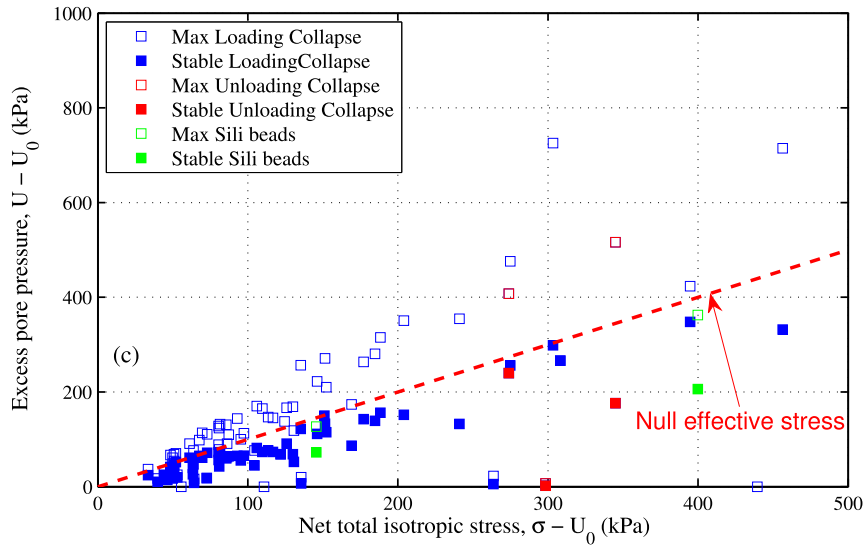
**Fig. 7.** Effects of $\sigma'_{3\text{trig}}$ on the excess pore pressure in isotropic collapses. Hollow (respt full) symbols indicate the maximum value obtained during (respt at the end) the transient phase *I*.
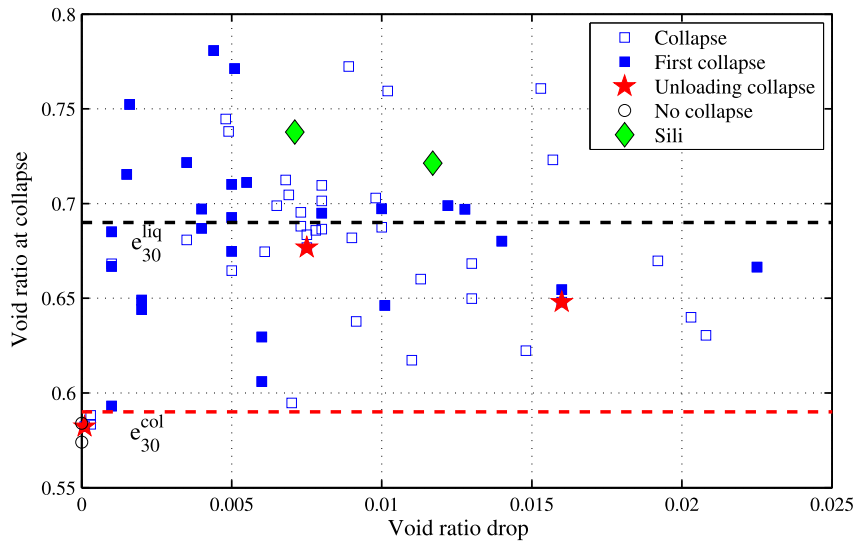


**Fig. 8.** Identification of the threshold void ratio $e_{30}^{\text{col}}$ indicating a total disappearance of dynamic collapses on dense samples.

Germany[2]). Neither grain breakage nor doublet of welded grains was found in binocular microscopy after testing; however, global liquefaction and unloading collapse happen in some rare cases.

### 3.3. Structural instability hypothesis

Theoretically, an isotropic compression on a linear isotropic medium can only result in an isotropic strain. For a granular medium, an isotropic strain does not modify significantly the relative position of the grains. However, in our experiments, it has been observed that the strain is strongly anisotropic, resulting in a large rearrangement of the grain structure. Since the preferential force chains carry most of the applied stress in a granular assembly [16–18], it is *hypothesized* that under isotropic stress solicitation, the induced strain can be strongly anisotropic due to the initial structural anisotropy despite the observed quasi-elastic behaviour. This initial structural anisotropy of an assembly of spherical particles could result from a preferred orientation of unit vectors normal to contact surfaces [19] and be a major ingredient in generating the observed collapses. The rapid pore-pressure fluctuations can be originated in the micro-structural instability resulting from the local

---

[2] www.sigmund-lindner.com.
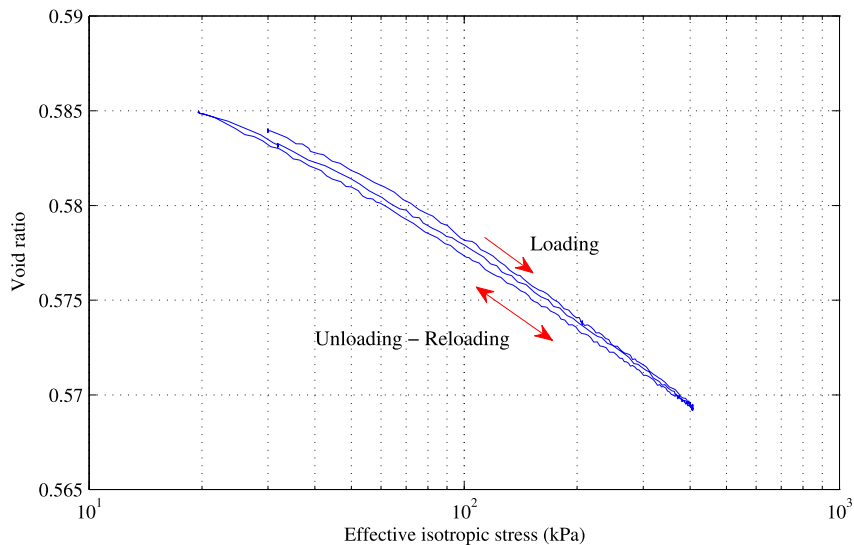
**Fig. 9.** Collapse-free behaviour on dense model granular sample during some isotropic cycles between 20 and 400 kPa, $e_{30} = 0.584$ (Dr $= 91.1\%$), created by the dry deposition method. A particularly quasi-elastic behaviour with the compression index $C_s = 0.0156 \approx$ the swelling index $C_c = 0.0137$ is observed.

collapse of the contact network and subsequent rapid rearrangements of a metastable structure. The sudden breakage of these chains is facilitated by rolling of perfect spherical grain shape, as noticed in recent experiments [20]. This can induce local dynamic shear deformation, and result in a fast pore water pressure buildup due to the incompressibility of water in a fully saturated media. Consequently, the pore fluid is not the cause of the observed collapses. It is responsible only for amplification of the event, and more precisely for their consequences, like partial liquefaction or even full liquefaction [12]. A large $\Delta U$ can decrease the grain-contact stresses towards a possible vanishing stress state and increase the axial and volumetric strain [21]. Using this hypothesis, isotropic instabilities and shear stick-slips can probably share the same physical origin. The local or global failure of the contact network would explain the larger magnitudes of the collapse in saturated samples [9,11], compared to dry ones [8], and the spontaneity of slip events in the experimental works [22–24].

## 4. Conclusions

The spontaneous instabilities of fully saturated model granular materials under isotropic consolidation have been reported in this paper. These instabilities are reflected in local collapses and partial liquefaction. This collapsibility, characterized by an overpressure of interstitial pore fluid, is probably an essential feature of the spherical shape of glass beads. It can be a clue to the physical cause beneath the strange observed instabilities. However, how the excess pore pressure is generated, propagated and maintained is still a mystery. The sudden rearrangements of the metastable anisotropic microstructure resulting from the local collapse of contact networks could be the mechanism. This paper also reveals that no collapse occurs for dense samples below a threshold void ratio $e_{30}^{col}$. However, the effects of sample size and the particle size distribution on this threshold void ratio remain unknown. These unexpected collapses, especially in isotropic unloading, represent a new challenge for both theoretical soil mechanics and numerical discrete element modelling. Up to now, isotropic collapses have never been observed on natural granular materials. The existence of isotropic collapsibility on real sands in nature remains quite speculative. However, this phenomenon may exist, but just needs to be discovered.

## Acknowledgements

## References

[1] D.M. Wood, General report: evaluation of material properties, in: S.M.S. Shibuya, T. Mitachi (Eds.), Proc. Pre-failure Deformation of Geomaterials, vol. 2, Sapporo, Japan, Rotterdam, Balkema, 1994, pp. 117–1199.
[2] K. Terzaghi, R.P. Peck, G. Mesri, Soil Mechanics in Engineering Practice, 3rd edition, John Wiley, 1996.
[3] I. Herle, G. Gudehus, Determination of parameters of a hypoplastic constitutive model from properties of grain assemblies, Mech. Cohes.-Frict. Mater. 4 (5) (1999) 461–486.
[4] C. O'Sullivan, Particulate Discrete Element Modelling, Spon Press, 2011.
[5] F. Radjaï, F. Dubois, Discrete Numerical Modeling of Granular Materials, Wiley, 2011.
[6] P.A. Cundall, O.D.L. Strack, A discrete numerical model for granular assemblies, Geotechnique 29 (47) (1979) 47–65.
[7] C. Thornton, Numerical simulations of deviatoric shear deformation of granular media, Geotechnique 50 (43) (2000) 43–53.
[8] F. Adjemian, P. Evesque, Experimental study of stick-slip behaviour, Int. J. Numer. Anal. Methods Geomech. 28 (6) (2004) 501–530.

[9] K.A. Alshibli, L.E. Roussel, Experimental investigation of stick-slip behaviour in granular materials, Int. J. Numer. Anal. Methods Geomech. 30 (14) (2006) 1391–1407.

[10] A.F. Çabalar, C.R.I. Clayton, Some observations of the effects of pore fluids on the triaxial behaviour of a sand, Granul. Matter 12 (1) (2010) 87–95.

[11] T. Doanh, M.T. Hoang, J.-N. Roux, C. Dequeker, Stick-slip behaviour of model granular materials in drained triaxial compression, Granul. Matter 15 (1) (2013) 1–23.

[12] T. Doanh, A. Le Bot, N. Abdelmoula, S. Hans, C. Boutin, Liquefaction of immersed granular media under isotropic compression, Europhys. Lett. 108 (2014) 24004.

[13] D.M. Wood, Soil Behaviour and Critical State Soil Mechanics, Cambridge University Press, 1990.

[14] B. Andreotti, Y. Forterre, O. Pouliquen, Granular Media: Between Fluid and Solid, Cambridge University Press, 2013.

[15] Z. Finge, T. Doanh, Ph. Dubujet, Undrained anisotropy of Hostun RF loose sand: new experimental hints, Can. Geotech. J. 43 (11) (2006) 1195–1212.

[16] A. Drescher, G. De Josselin de Jong, Photoelastic verification of a mechanical model for the flow of a granular material, J. Mech. Phys. Solids 20 (1972) 337–351.

[17] C.H. Liu, S.R. Nagel, D.A. Schecter, S.N. Coppersmith, S. Majmudar, Force fluctuations in bead packs, Science 269 (1995) 513–515.

[18] D.M. Wood, D. Lesniewska, Stresses in granular materials, Granul. Matter 13 (2011) 395–415.

[19] M. Oda, K. Iwashita, Mechanics of Granular Materials: An Introduction, CRC Press, 1999.

[20] J. Wenzl, R. Seto, M. Roth, H.-J. Butt, G.K. Auernhammer, Measurement of rotation of individual spherical particles in cohesive granulates, Granul. Matter 15 (2013) 391–400.

[21] A. Kabla, G. Debrégeas, Contact dynamics in a gently vibrated granular pile, Phys. Rev. Lett. 92 (2004) 035501.

[22] S. Nasuno, A. Kudrolli, J.P. Gollub, Friction in granular layers: hysteresis and precursors, Phys. Rev. Lett. 79 (1997) 949–952.

[23] J.C. Géminard, W. Losert, J.P. Gollub, Frictional mechanics of wet granular material, Phys. Rev. E, Stat. Nonlinear Soft Matter Phys. 59 (1999) 5881.

[24] J.-C. Tsai, G.A. Voth, J.P. Gollub, Internal granular dynamics, shear-induced crystallization, and compaction steps, Phys. Rev. Lett. 91 (2003) 064301.